Volume 67, Issue 3, 2023
Journal of Scientific Research
of
The Banaras Hindu University

Designing an Air Core Photonic Bandgap Fiber to Study the Dispersion and Loss Characteristics for Optical Pulse Propagation

Devika Phukan*[1], Priyanka Talukdar[2], and Pranami Sarma[3]

*[1]Department of Physics, Royal Global University, Guwahati 781035, Assam, mail id: devikaphukan@gmail.com

[2]Department of Physics, Royal Global University, Guwahati 781035, Assam, mail id: priyankatalukdar17031995@gmail.com

[3]Department of Physics, Royal Global University, Guwahati 781035, Assam, mail id: sarmapranami37@gmail.com

Abstract

The wavelength dependence of the Group velocity dispersion (GVD) in an air core Photonic Bandgap fiber (PBGF) with 9 air hole rings has been investigated. The waveguide GVD of the designed fiber is studied and found that the GVD strongly depends on the structure and geometrical parameters of the fiber. It is strongly affected by photonic bandgap edges at the bandwidth boundaries due to the confinement of light by the photonic band gap effect. It is seen that the GVD value shifts from negative at shorter wavelengths to positive values at longer wavelengths and the zero-dispersion wavelength could be changed by changing the hole diameter to pitch ratio.

Keywords: Bandwidth, Dispersion, Group velocity dispersion, leakage loss, Photonic Band-gap fiber, photonic band gap effect,

I. Introduction

A typical air core Photonic Bandgap fiber (PBGF) comprises one to two hundred wavelength-scale air holes, normally with a very high air filling factor, arranged in a 2-D array that is maintained along the full length of the fiber [1]. The cladding region of a Photonic Bandgap fiber is generally made up of a periodic arrangement of air holes. Light propagates along the fiber length in the low index core region [2]. The core of an air core PBGF is formed by removing several unit cells from the cladding of the fiber. Light can be guided through this central air hole due to the photonic bandgap of the surrounding matrix [3]. Direct leakage of light from the core is reduced due to the incorporation of enough holes in the cladding in these fibers [4]. Recent reports have shown that dispersion characteristics of PBGF exhibit few unusual properties [5]. Usually, a cladding structure with triangular structure is used in PBGFs because of its large band gaps. It has been already experimentally demonstrated that triangular based PBGF exhibits guided mode confined in air in contrast to honeycomb based PBGF [6]. Though most research on PBGF have focused on triangular lattice cladding structure, a few studies have even shown the potential application of a square lattice cladding structure for generation of a photonic bandgap suitable for air guidance [7],[8],[9]. Air core PBGFs shows exceptionally low loss transmission, low nonlinearity, high power pulse delivery, a unique bandgap guiding mechanism and are able to guide over a wide spectral region which is why they have attained significant attention recently in fiber optic communication. These fibers can be designed to attain zero dispersion wavelengths at desired wavelengths and can outperform conventional optical fibers in various applications like supercontinuum generation, biomedical sensing, industrial equipment, etc. because most of the power is confined within the core and is delivered in a single mode [10],[11]. Because of the various refractive indices of different wavelengths, group velocity

DOI: 10.37398/JSR.2023.670306

dispersion (GVD) arise which results in limitation of data rate due to pulse broadening. The propagation of light is strongly wavelength dependent because PBGFs are resonant structures. The analysis of the waveguide dispersion provides a physical insight into the signal propagation mechanism in these fibers and hence is very important to understand for any optical transmission applications [12]. Short and high-power pulses are torn apart in conventional optical fibers because of self-phase modulation and Raman scattering. Studies have demonstrated that this problem can be solved using PBGFs which can be used to deliver high power ultrashort optical pulses without significant temporal distortion for relatively longer distance [13]. Dispersion characteristics and its control play an important role in optical communication systems. The control of dispersion in these microstructure fibers has been realised [14], [15]. Tailoring of zero dispersion wavelength by changing the diameter of air holes, pitch, refractive index normalised thickness of core rings and hole diameter to pitch ratio has been investigated [16].

Regarding experimental works, large core multimode 19 cell hollow core photonic bandgap fiber (HC-PBGF) has been fabricated using stack and draw technique and reported with a record combination of low loss (3.5 dB/km) and a wide 3 dB bandwidth at 1500 nm. The fabricated fiber showed ~1.46 times faster signal propagation than in conventional fiber which is a great feature for low latency telecommunication systems [17]. A 11 km long HC-PBGF characterized by a longitudinally uniform loss of ~5 dB/km loss at 1560 nm and a very broad transmission bandwidth has been experimentally demonstrated by a two-stage stack and draw technique. This was the first ever reported fabrication of greater than 10 km length of high-performance HC-PBGF with error free, low latency 10 Gbit/s transmission across the entire C band [18]. A 37 cell HC-PBGF has been fabricated and a low minimum fundamental mode loss of 3.3 dB/km at 1550 nm and an 85 nm wide bandwidth was presented which transmitted a total data rate of 73.7 Tb/s, setting a new transmission capacity target for HC-PBGFs [19]. Fabrication and characterisation of a 19 cell HC-PBGF operating in the mid Infrared has been reported that provides low loss guidance between 3.1 μm and 3.7 μm with a record of minimum attenuation of 0.12 dB/m at 3.33 μm and an extremely low bend loss of less than 0.25 dB per 5 cm diameter turn over a 300 nm bandwidth [20]. A simple tellurite PBGF with one array of high index rings in the cladding has been proposed and fabricated that can support the near and mid infra-red light transmitting in the core and can be used as a filter. This fiber can be widely applied in photon device fields, such as wavelength conversion, switching and mid infrared highly nonlinear devices [21]. A hybrid model of polarisation maintaining fiber based on the combination of photonic bandgap and anti-resonant effect has been presented. The main characteristics of these hybrid fibers are high birefringence and wide single mode bandwidth [22]. Synchronization of the cellular base station using emerging forms of hollow core fiber have been demonstrated which is possible because of their excellent thermal stability of propagation delay. This has led to a drastic reduction of the synchronisation error and represents a 20 times better improvement over standard single mode fiber system that is essential for applications like autonomous vehicle navigation, indoor localisation and most importantly, for high accuracy positioning in 5G networks [23]. By structural development and fabrication process optimisation, the losses of PBGFs can be reduced further. The present study tries to exhibit the propagation mechanism of an air core PBGF and explain its GVD and loss characteristics.

II. Proposed Fiber Structure:

The fiber considered is an air-core PBGF fabricated with finite number of air holes in triangular lattice with the background material silica which has a refractive index of 1.5. The air holes forming the inner ring has a centre-to-centre distance between holes of Λ= 2.8 μm, which is called the hole pitch. The air hole diameter is denoted as 'd' and the hole pitch is denoted as 'Λ'. Perfectly matched layers (PMLs) are used as the boundary condition as shown in figure 1. The field considered is Gaussian and the number of air hole ring considered is finite.

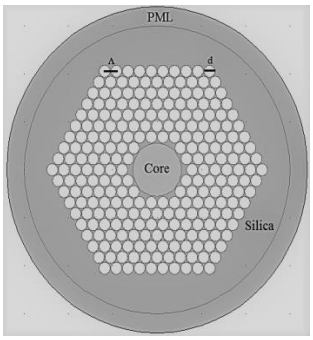

Figure 1: Pictorial representation of an air core PBGF with background material silica and perfectly matched layer (PML) as boundary condition

III. Optical Simulations and discussions:

The total dispersion D (λ) can be calculated as the sum of waveguide dispersion D_w (λ) and material dispersion D_m (λ), which can be expressed as

$$\boldsymbol{D\ (\lambda) = D_w(\lambda) + D_m(\lambda)} \quad \textbf{(1)}$$

$$\boldsymbol{D_w(\lambda) = -\frac{\lambda}{c}\frac{d^2}{d\lambda^2} Re\ (n_{eff})} \quad \textbf{(2)}$$

$$\boldsymbol{D_m\ (\lambda) = -\frac{\lambda}{c}\frac{d^2 n_m}{d\lambda^2}} \quad \textbf{(3)}$$

Where, λ is the wavelength, D(λ) is the total dispersion, D_w(λ) is the waveguide dispersion, D_m(λ) is the material dispersion, n_{eff} is the effective index, n_m is refractive index estimated by using Sellmeier equations [24],[25] and c represents speed of light.

The leakage loss, L_c, also called the confinement loss, is a significant parameter of PBGFs with a finite number of air holes. When considering a PBGF with infinite number of air holes, light remains confined in the core region by a fully two-dimensional photonic bandgap and hence there is no leakage loss [26]. But, the number of air holes cannot be infinite when a fiber is fabricated, so the mode is leaky in practical and leakage loss occurs, which is derived from the attenuation constant 'α' as

$$\boldsymbol{L_c = 8.86\ \alpha} \quad \textbf{(4)}$$

The simulations are done using the Finite Difference Time Domain (FDTD) method. The FDTD method can be applied predominantly for solving complex electromagnetic computations. The FDTD algorithm has turned out to be a major appliance in nanophotonic over the past decade because of its ability to deal with complex structures [27]. The integrated design of this simulator provides scripting capability, advanced post processing through various time and frequency profile monitors, optimizations, sweeps, far field analysis, modal analysis, and many more such options, enabling designers to accurately design various models. This method simulates the set of Maxwell's equations evolving with time by using the finite difference approximation and divides space and time into a regular grid [28]. The resulting equations are solved in a loop method. The FDTD method applies the finite difference approximation to convert the Maxwell's equations into a numerical Eigen value problem. The mode propagation constant, ß can be obtained from the updated equations. The eigen value equations can be solved to determine ß, for a considered geometry of the HC-PCF [29]. The effective index (n_{eff}) of the mode can be calculated by the equation.

$$\boldsymbol{n_{eff} = \beta/k_0} \quad \textbf{(5)}$$

Where ß is the propagation constant and k_0 is the angular wave number. FDTD provides various simulation objects to define simulation parameters like mesh size and boundary conditions. FDTD also introduces conformal mesh technology that can be used to improve simulation accuracy. There is different time and frequency domain monitors to visualize results of the simulation. Conformal mesh refinement is applied to the simulations done in the present study to approach precise measurements and to diminish errors.

The dispersion and dispersion slope are important characteristics of PBGFs that can limit the useful spectral bandwidth of the fiber. The modal dispersion curve is shown in figure 2 as a function of normalised wavelength, λ/ʌ, with 9 number of air hole rings in the fiber. We have considered two PBG boundaries, one with d/ʌ =0.7 and the other with d/ʌ = 0.75. The dashed line here shows the modal dispersion curve, and the solid lines indicate PBG boundaries (upper and lower bandgap edges). The fundamental mode remains inside the Photonic bandgap region. The width of the bandgap becomes narrower with the decrease in d/ʌ value. This happens because with the decrease in d/ʌ, air filling fraction becomes small and with different d/ʌ values, the cut-off wavelength varies. The PBGF with d/ʌ =0.75 has the fundamental mode in the shorter wavelength region and covers a wider wavelength range. The PBGF with d/ʌ =0.7 has the fundamental mode in the longer wavelength region and covers a comparatively narrower wavelength range. With the increase in the hole pitch value, the modal dispersion curve gets more flattened, and the bandgap moves towards the longer wavelength region. This shows the significant effect of the hole pitch on the bandgap of the fiber. The lower and higher cut-off wavelength for d/ʌ = 0.75 are λ/ʌ = 0.462 and λ/ʌ =0.548 respectively. For d/ʌ =0.7, the lower and higher cut-off wavelengths are λ/ʌ = 0.584 and λ/ʌ =0.636.

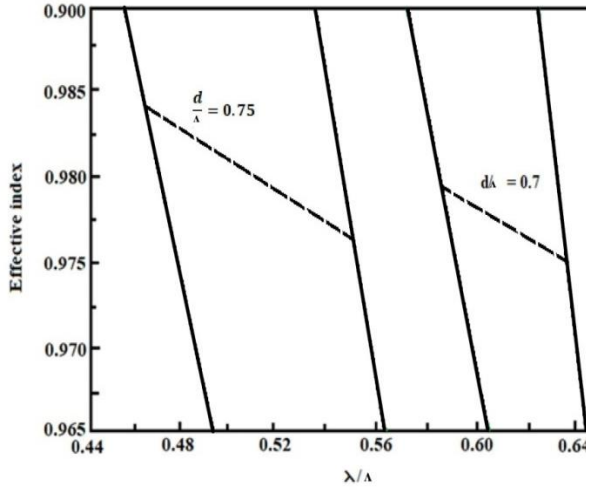

Figure 2*: Modal dispersion curve as a function of normalized wavelength for the air core PBGF with two values of d/Λ=0.7 and d/Λ=0.75*

Next, we consider the air hole size effect on dispersion. Taking Λ= 2.80 μm, we have varied the air hole size from 1.96 μm to 2.16 μm. We have considered 9 air hole rings in the cladding region of the fiber and increased the air hole to pitch ratio (d/Λ) from 0.7 to 0.75. The proposed fiber shows unusual and wide waveguide group velocity dispersion. (fig 3) The GVD is prominent in the upper and lower band edges rather than in the centre region. The PBGF with large value of d/Λ has a smaller slope around the centre of photonic bandgap than the PBGF with smaller d/Λ. GVD is strongly wavelength dependent in nature, and it shifts from negative to positive values as it goes from shorter to longer wavelength. The GVD increases swiftly around the upper band edge and decreases swiftly near the lower band edge. With the decrease in d/Λ, the position of zero dispersion wavelength shifts towards longer wavelength, the width of bandgap becomes narrower and the dispersion slope at the centre of photonic bandgap and at the band gap edges becomes steeper.

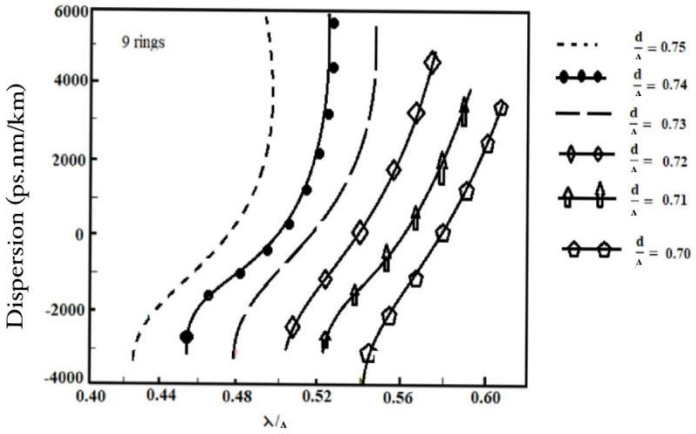

Figure 3: *Normalised Waveguide group velocity dispersion of an air core PBGF with 9 rings of air holes taking hole diameter to pitch ratio as the parameter.*

The leakage loss decreases regularly with increase in the number of rings.(fig 4) At least 22 rings are needed to minimize the leakage loss to 10^{-2} dB/m in 1.5 μm wavelength region when using air hole diameter to pitch ratio of 0.7. It is observed that 22 rings minimize the leakage loss to 10^{-2} dB/m in 1.5 μm wavelength region when using air hole diameter to pitch ratio of 0.7. But its fabrication needs significant attention for practical covering.

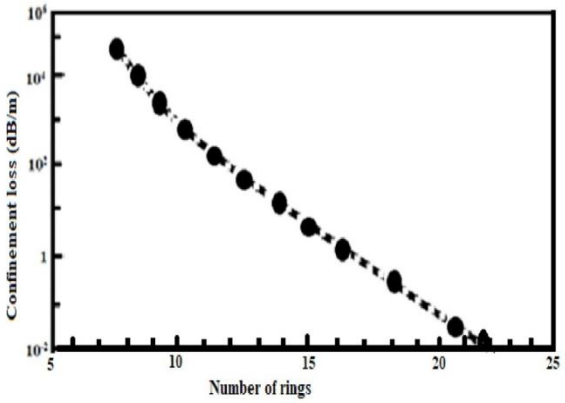

Figure 4: *Leakage loss (dB/m) as a function of number of rings with d/Λ = 0.7 and λ= 1.5 μm*

Figure 5 shows the Normalised leakage loss of the PBGF with 9 rings of air holes, taking hole diameter to pitch ratio as the parameter. With the increase in the hole diameter to pitch ratio, the leakage loss decreases extremely. Taking finite number of air hole rings in the cladding, d/Λ value should be large enough to reduce the leakage loss in an air core

PBGF. Using d/ʌ= 0.75 and ʌ= 2.80 μm, leakage loss of 10^{-2} dB/m can be realised in 1.5 μm region.

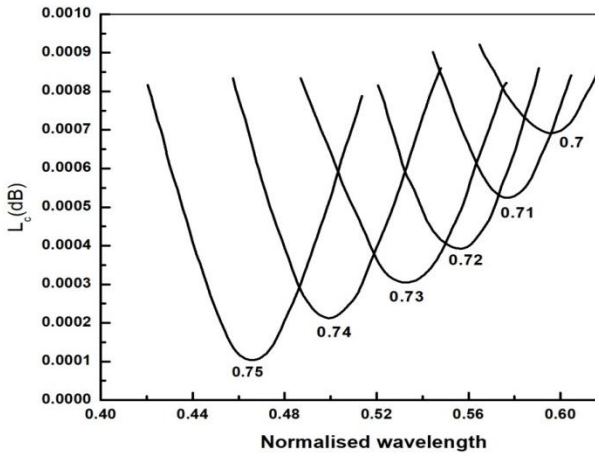

Figure 5: *Normalised leakage loss as a function of normalised wavelength with hole diameter to pitch ratio (d/ʌ) as the parameter*

Photonic Bandgap fibers have now been realised as a versatile tool in the field of optical fiber communication technology because of their unique optical properties that are not possible to achieve for applications in conventional fibers. The key properties of these fibers like low latency, higher damage thresholds, lower nonlinearity, low confinement or leakage loss and high transmission capacity opens up a host of potential application options, like intra and inter data centre interconnection, long haul optical communications, gas-sensing and gas-based nonlinear optics.

IV. Conclusion

A physical view into the propagation mechanism of an air core photonic bandgap fiber has been presented to understand optical pulse transmission applications. The effect of various geometrical parameters like air hole diameter, hole pitch and number of air hole rings is investigated to show how these parameters influence the dispersion and loss characteristics of the designed PBGF. The wavelength dependence of Group velocity dispersion of the designed PBGF is studied and it is seen that the GVD value shifts from negative at shorter wavelengths to positive values at longer wavelengths. The waveguide GVD changes rapidly near the band edge and have a slow variance near the centre due to the photonic bandgap effect. The photonic bandgap grows wider with the increase in air hole diameter. The zero-dispersion wavelength can be changed by changing the hole diameter to pitch ratio. It is observed that the PBGF with large value of hole diameter to pitch ratio has a smaller slope around the centre of photonic bandgap than the PBGF with smaller hole diameter to pitch ratio. The influence of the cladding ring numbers on leakage loss was explored. The leakage loss was seen decreasing regularly with increase in the number of rings and it is observed that with the increase in the hole diameter to pitch ratio, the leakage loss decreases randomly. But its fabrication needs to be significantly studied for implimentaion in practical field.The report presents advantages of using air core PBGF as a medium for transmission of optical pulse.

Sl no.	λ/Λ (d/Λ=0.75)	Effective Index	λ/Λ (d/Λ=0.7)	Effective Index
1	0.461	0.915	0.584	0.926
2	0.468	0.917	0.589	0.927
3	0.476	0.918	0.594	0.929
4	0.483	0.920	0.601	0.931
5	0.489	0.921	0.605	0.932
6	0.496	0.923	0.609	0.933
7	0.501	0.924	0.613	0.934
8	0.508	0.926	0.617	0.935
9	0.515	0.927	0.620	0.936
10	0.522	0.929	0.623	0.937
11	0.528	0.930	0.625	0.938
12	0.535	0.932	0.629	0.939
13	0.540	0.933	0.633	0.940
14	0.544	0.934	0.636	0.941
15	0.548	0.935	0.637	0.942

Table 1: Table for Modal dispersion curve as a function of normalized wavelength for the air core PBGF with two values of d/Λ=0.75 and d/Λ=0.7 with respect to figure 2

Sl no	λ/Λ (X-Axis)	Dispersion (ps/nm.km) (d/Λ=0.75) (Y-Axis)	λ/Λ (X-Axis)	Dispersion (ps/nm.km) (d/Λ =0.74) (Y-Axis)	λ/Λ (X-Axis)	Dispersion (ps/nm.km) (d/Λ =0.73) (Y-Axis)	λ/Λ (X-Axis)	Dispersion (ps/nm.km) (d/Λ =0.72) (Y-Axis)	λ/Λ (X-Axis)	Dispersion (ps/nm.km) (d/Λ =0.71) (Y-Axis)	λ/Λ (X-Axis)	Dispersion (ps/nm.km) (d/Λ =0.7) (Y-Axis)
1	0.492	5806.20	0.519	5689.92	0.543	5612.40	0.568	5302.32	0.583	4527.13	0.599	4255.81
2	0.495	5263.56	0.523	4837.20	0.545	4992.24	0.566	4410.85	0.580	3790.69	0.597	3674.41
3	0.497	4798.44	0.524	4062.01	0.547	4100.77	0.565	3829.45	0.577	2976.74	0.594	3015.50
4	0.499	3713.17	0.525	3286.82	0.547	3325.58	0.563	3170.54	0.574	2317.82	0.591	2472.86
5	0.499	3131.78	0.524	2434.10	0.547	2627.90	0.560	2472.86	0.570	1697.67	0.587	1891.47
6	0.495	2007.75	0.522	1775.19	0.545	2007.75	0.555	1736.43	0.566	1116.27	0.582	1155.03
7	0.493	1503.87	0.519	1116.27	0.541	1348.83	0.549	922.48	0.562	689.92	0.577	496.12
8	0.489	999.99	0.513	534.88	0.533	883.72	0.543	341.08	0.558	186.04	0.572	-162.79
9	0.479	302.32	0.503	31.00	0.527	418.60	0.533	-240.31	0.551	-240.31	0.566	-705.42
10	0.474	31.00	0.491	-395.34	0.517	-7.75	0.523	-666.66	0.544	-550.38	0.559	-1209.30
11	0.468	-162.79	0.480	-744.18	0.506	-550.38	0.514	-1131.78	0.536	-1054.26	0.554	-1635.65
12	0.455	-627.90	0.470	-1054.26	0.494	-1054.26	0.508	-1558.14	0.528	-1596.89	0.548	-2023.25
13	0.450	-821.70	0.458	-1519.38	0.485	-1713.17	0.505	-1984.49	0.524	-2178.29	0.544	-2527.13
14	0.436	-1519.38	0.451	-2255.81	0.478	-2488.37	0.501	-2604.65	0.521	-2643.41	0.542	-3031.00
15	0.431	-1984.49	0.447	-3108.52	0.543	5612.40	0.498	-3069.76	0.516	-3147.28	0.538	-3651.16

Table 2: Table for Normalised Waveguide group velocity dispersion of an air core PBGF with 9 rings of air holes taking hole diameter to pitch ratio as the parameter with respect to figure 3 (d/Λ=0.75,0.74,0.73,0.72,0.71,0.7)

Sl No.	No. of rings	Leakage loss (dB/m)
1	7	946107.756
2	8	838323.383
3	9	742514.9877
4	10	670658.6627
5	11	598802.3377
6	12	538922.1049
7	13	485029.9183
8	14	419161.6394
9	15	365269.4527
10	16	323353.3583
11	17	269461.1717
12	18	215568.8708
13	19	179640.8225
14	20	89820.47336
15	21	71856.33501
16	22	47904.03632

Table 3: Leakage loss as a function of number of rings with d/ʌ= 0.7 and λ=1.5 μm with respect to figure 4

Sl No	λ/ʌ (X-Axis)	L_c (dB) (d/ʌ=0.75) (Y-Axis)	λ/ʌ (X-Axis)	L_c (dB) (d/ʌ =0.74) (Y-Axis)	λ/ʌ (X-Axis)	L_c (dB) (d/ʌ =0.73) (Y-Axis)	λ/ʌ (X-Axis)	L_c (dB) (d/ʌ =0.72) (Y-Axis)	λ/ʌ (X-Axis)	L_c (dB) (d/ʌ =0.71) (Y-Axis)	λ/ʌ (X-Axis)	L_c (dB) (d/ʌ =0.7) (Y-Axis)
1	0.420	8.1E-4	0.457	8.3E-4	0.487	8.3E-4	0.525	7.26E-04	0.549	8.34E-04	0.571	8.51E-04
2	0.425	7.2E-4	0.458	7.9E-4	0.489	7.9E-4	0.528	6.71E-04	0.551	8.01E-04	0.575	8.09E-04
3	0.427	6.8E-4	0.461	7.5E-4	0.492	7.4E-4	0.532	5.99E-04	0.554	7.53E-04	0.579	7.70E-04
4	0.431	5.9E-4	0.466	6.4E-4	0.500	6.3E-4	0.536	5.45E-04	0.556	7.17E-04	0.584	7.36E-04
5	0.436	4.9E-4	0.468	5.9E-4	0.505	5.5E-4	0.540	4.84E-04	0.558	6.85E-04	0.581	7.21E-04
6	0.439	4.4E-4	0.472	5.2E-4	0.510	4.8E-4	0.546	4.25E-04	0.561	6.45E-04	0.89	7.09E-04
7	0.446	2.9E-4	0.477	4.4E-4	0.515	4.1E-4	0.555	3.93E-04	0.564	6.00E-04	0.591	7.01E-04
8	0.449	2.5E-4	0.481	3.6E-4	0.529	3.0E-4	0.561	4.03E-04	0.569	5.56E-04	0.597	6.93E-04
9	0.452	1.9E-4	0.485	3.0E-4	0.537	3.1E-4	0.566	4.41E-04	0.575	5.27E-04	0.603	7.10E-04
10	0.472	1.2E-4	0.501	2.1E-4	0.547	3.8E-4	0.571	4.91E-04	0.582	5.35E-04	0.607	7.39E-04
11	0.486	2.7E-4	0.512	2.8E-4	0.561	5.8E-4	0.573	5.36E-04	0.587	5.76E-04	0.610	7.82E-04
12	0.490	3.5E-4	0.516	3.3E-4	0.566	6.5E-4	0.577	5.99E-04	0.591	6.31E-04	0.614	8.19E-04
13	0.496	4.5E-4	0.523	4.3E-4	0.570	7.2E-4	0.584	7.13E-04	0.598	7.34E-04	0.617	8.57E-04
14	0.501	5.4E-4	0.527	5.0E-4	0.573	7.7E-4	0.586	7.65E-04	0.601	7.85E-04	0.619	8.90E-04
15	0.505	6.2E-4	0.545	8.3E-4	0.575	8.0E-4	0.589	8.17E-04	0.605	8.41E-04	0.621	9.32E-04

Table 4: Normalised leakage loss as a function of normalised wavelength with hole diameter to pitch ratio (d/ʌ) as the parameter with respect to figure 5

References

1. Poletti, F., Petrovich, M. N., & Richardson, D. J. (2013). Hollow-core photonic bandgap fibers: technology and applications. *Nanophotonic*, *2*(5-6), 315-340.
2. Murao, T., Saitoh, K., & Koshiba, M. (2006). Design of air-guiding modified honeycomb photonic band-gap fibers for effective single-mode operation. *Optics express*, *14*(6), 2404-2412.
3. Birks, T. A., Roberts, P. J., Russell, P. S. J., Atkin, D. M., & Shepherd, T. J. (1995). Full 2D photonic band gaps in silica/air

structures. *Electronics letters*, *31*(22), 1941-1943.

4. West, J. A., Smith, C. M., Borrelli, N. F., Allan, D. C., & Koch, K. W. (2004). Surface modes in air-core photonic band-gap fibers. *Optics Express*, *12*(8), 1485-1496.
5. Khatak, S., & Singh, G. P. (2018). Dispersion Management in Photonic Crystal Fibers. International Journal of Electronics Engineering, 10(1), 146-152
6. Cregan, R. F., Mangan, B. J., Knight, J. C., Birks, T. A., Russell, P. S. J., Roberts, P. J., & Allan, D. C. (1999). Single-mode photonic band gap guidance of light in air. *science*, *285*(5433), 1537-1539.
7. Chen, M. Y., & Yu, R. (2004). Square-structured photonic bandgap fibers. *Optics communications*, *235*(1-3), 63-67.
8. Buczynski, R., Pysz, D., Ritari, T., Szarniak, P., Saj, W., Kujawa, I., & Stepien, R. (2005). Hollow-core photonic crystal fiber with square lattice. In *Photonic Crystals and Fibers* ,5950, 270-277
9. Zhang, H., Wang, Q., Yang, B., & Yu, L. (2008). Dispersion properties of hollow-core photonic bandgap fibers based on a square lattice cladding. *Optics communications*, *281*(13), 3486-3491.
10. Hassan, Q. M., Raheem, N. A., Emshary, C. A., Dhumad, A. M., Sultan, H. A., & Fahad, T. (2022). Preparation, DFT and optical nonlinear studies of a novel azo-(β)-diketone dye. *Optics & Laser Technology*, *148*, 107705.
11. Shephard, J. D., Jones, J. D. C., Hand, D. P., Bouwmans, G., Knight, J. C., Russell, P. S. J., & Mangan, B. J. (2004). High energy nanosecond laser pulses delivered single-mode through hollow-core PBG fibers. *Optics Express*, *12*(4), 717-723.
12. Jasapara, J., Her, T. H., Bise, R., Windeler, R., & DiGiovanni, D. J. (2003). Group-velocity dispersion measurements in a photonic bandgap fiber. *JOSA B*, *20*(8), 1611-1615.
13. Ortigosa-Blanch, A., Knight, J. C., Wadsworth, W. J., Arriaga, J., Mangan, B. J., Birks, T. A., & Russell, P. S. J. (2000). Highly birefringent photonic crystal fibers. *Optics letters*, *25*(18), 1325-1327.
14. Lægsgaard, J., Roberts, P. J., & Bache, M. (2007). Tailoring the dispersion properties of photonic crystal fibers. *Optical and Quantum Electronics*, *39*, 995-1008.
15. Humbert, G., Knight, J. C., Bouwmans, G., Russell, P. S. J., Williams, D. P., Roberts, P. J., & Mangan, B. J. (2004). Hollow core photonic crystal fibers for beam delivery. *Optics express*, *12*(8), 1477-1484.
16. Hu, Z., Bo-Jun, Y., Yu-Min, L., Qiu-Guo, W., Li, Y., & Xiao-Guang, Z. (2009). Zero dispersion wavelength and dispersion slope control of hollow-core photonic bandgap fibres. *Chinese Physics B*, *18*(3), 1116.
17. Wheeler, N. V., Petrovick, M. N., & Slavik, R. (2012). Nonlinear optics in optical fiber technology. In Proceedings of the National Fiber Optic Engineers Conference. Optica Publishing Group.
18. Chen, Y., Liu, Z., Sandoghchi, S. R., Jasion, G., Bradley, T. D., Numkam, E., ... & Richardson, D. J. (2015, March). Demonstration of an 11km hollow core photonic bandgap fiber for broadband low-latency data transmission. In *Optical Fiber Communication Conference* (Th5A-1). Optica Publishing Group.
19. Sleiffer, V. A., Jung, Y., Baddela, N. K., Surof, J., Kuschnerov, M., Veljanovski, V., ... & de Waardt, H. (2013). High capacity mode-division multiplexed optical transmission in a novel 37-cell hollow-core photonic bandgap fiber. *Journal of lightwave technology*, *32*(4), 854-863.
20. Petrovich, M. N., Heidt, A. M., Wheeler, N. V., Baddela, N. K., & Richardson, D. J. (2014, June). High sensitivity methane and ethane detection using low-loss mid-IR hollow-core photonic bandgap fibers. In *23rd International Conference on Optical Fibre Sensors* (Vol. 9157, pp. 521-524). SPIE.
21. Cheng, T., Duan, Z., Liao, M., Gao, W., Deng, D., Suzuki, T., & Ohishi, Y. (2013). A simple tellurite photonic bandgap fiber based on one array of rings. In *2013 Conference on Lasers and Electro-Optics Pacific Rim (CLEOPR)* (1-2). IEEE.
22. Guo, Y., Wang, X., Xing, Z., & Lou, S. (2021). Hybrid hollow-core polarization-maintaining fiber with high birefringence and wide single mode bandwidth. *Results in Physics*, *29*, 104725.
23. Zhu, W., Fokoua, E. R. N., Chen, Y., Bradley, T. D., Sandoghchi, S. R., Ding, M., ... & Slavík, R. (2019). Toward high accuracy positioning in 5G via passive synchronization

of base stations using thermally-insensitive optical fibers. *IEEE Access*, *7*, 113197-113205.

24. Hussein, R. A., Hameed, M. F. O., & Obayya, S. S. (2015). Ultrahigh soliton pulse compression through liquid crystal photonic crystal fiber. *IEEE Journal of Selected Topics in Quantum Electronics*, *22*(2), 302-309.
25. Coscelli, E., Poli, F., Li, J., Cucinotta, A., & Selleri, S. (2015). Dispersion engineering of highly nonlinear chalcogenide suspended-core fibers. *IEEE PHOTONICS JOURNAL*, *7*(3), 1-8.
26. Saitoh, K., & Koshiba, M. (2003). Leakage loss and group velocity dispersion in air-core photonic bandgap fibers. *Optics Express*, *11*(23), 3100-3109.
27. Lesina, A. C., Vaccari, A., Berini, P., & Ramunno, L. (2015). On the convergence and accuracy of the FDTD method for nanoplasmonics. *Optics Express*, *23*(8), 10481-10497.
28. Oskooi, A. F., Roundy, D., Ibanescu, M., Bermel, P., Joannopoulos, J. D., & Johnson, S. G. (2010). MEEP: A flexible free-software package for electromagnetic simulations by the FDTD method. *Computer Physics Communications*, *181*(3), 687-702.
29. Pakarzadeh, H., Rezaei, S. M., & Namroodi, L. (2019). Hollow-core photonic crystal fibers for efficient terahertz transmission. *Optics Communications*, *433*, 81-88.